Polymer Chemistry

Accepted Manuscript

ROYAL SOCIETY OF CHEMISTRY

www.rsc.org/polymers

Zwitterionic poly(2-oxazoline)s as promising candidates for blood contacting applications

Lutz Tauhardt,[1,2] David Pretzel,[1,2] Kristian Kempe,[1,2,#] Michael Gottschaldt,[1,2] Ulrich S. Schubert*[1,2,3]

[1]Laboratory of Organic and Macromolecular Chemistry (IOMC), Friedrich Schiller University Jena, Humboldtstr. 10, 07743 Jena, Germany.

[2]Jena Center for Soft Matter (JCSM), Friedrich Schiller University Jena, Philosophenweg 7, 07743 Jena, Germany.

[3]Dutch Polymer Institute (DPI), John F. Kennedylaan 2, 5612 AB Eindhoven, The Netherlands.

[#]Current address: Department of Chemical and Biomolecular Engineering, The University of Melbourne, Victoria 3010, Australia.

Corresponding author footnote: Fax. +49 3641 948 202; Email: ulrich.schubert@uni-jena.de

Abstract:

We report the synthesis of highly hemo- and cytocompatible zwitterionic 2-oxazoline-based poly(sulfobetaine)s and poly(carboxybetaine)s, which demonstrate beneficial anticoagulant activity. The polymers were obtained by thiol-ene photoaddition of a tertiary amine-containing thiol onto an alkene-containing precursor copoly(2-oxazoline), followed by betainization with 1,3-propansultone and *β*-propiolactone. The polymers and their intermediates were characterized

by means of ^{1}H NMR spectroscopy and size exclusion chromatography. The influence of the zwitterionic polymers on the aggregation and hemolysis of erythrocytes, the whole blood viscosity, the platelet and complement activation as well as the blood coagulation has been studied in detail. In addition, the cytotoxicity of the materials has been evaluated. It was found that the zwitterionic POx show no negative interactions with blood. Moreover, anticoagulant activity *via* the intrinsic coagulation pathway was observed. The high hemocompatibilit and the low cytotoxicity as well as the beneficial anticoagulant activity of the presented zwitterionic poly(2-oxazoline)s demonstrate their potential for the use in biomedical applications.

Introduction

Zwitterionic polymers, also known as poly(betaine)s, are of significant interest as coating materials for medical devices, implants and drug delivery systems. Due to their hydrophilic, protein repellent character, they have been investigated as antifouling coatings for the reduction of non-specific adhesion and adsorption of proteins, microorganisms and eukaryotic cells.[1-4] The most prominent zwitterionic polymer is poly(2-methacryloyloxyethyl phosphorylcholine). It can be obtained by the controlled radical polymerization of the commercially available 2-methacryloyloxyethyl phosphorylcholine[5, 6] and is used as coating material, e.g., in contact lenses.[7, 8] Other widely-used zwitterionic polymers are poly(sulfobetaine)s and poly(carboxybetaine)s. Generally, they are obtained either by controlled radical polymerization of appropriate zwitterionic monomers, which are usually based on 2-(*N,N*-dimethylamino)ethyl methacrylate (DMAEMA),[1-4, 9-12] or by post-polymerization modification of poly(DMAEMA) (co)polymers.[13, 14] An outstanding property of these polymers is their excellent blood compatibility which, in some cases, is going along with an anticoagulant activity leading to a

prolongation of the blood clotting time.[10-12, 15, 16] This is important within medical applications where thrombogenicity is undesired.

In a dissolved state, anticoagulant polymers are of particular interest as heparin mimetics. Heparin, a well-known polysaccharide with multiple negative charges per repeating unit, is a widely used anticoagulant reagent for the treatment and prevention of thrombosis, which can result from operations, blood transfusions, or dialysis. However, being obtained from animal tissues sources, the use of heparin comes along with some problems, e.g. contaminations, a heterogeneous effectiveness depending on the isolated batches, and most importantly, heparin can lead to autoimmune diseases in long term treated patients.[17] Therefore, biocompatible anticoagulant polymers, which can be synthesized in a standardized procedure yielding products with identical chemical and functional characteristics, display a promising alternative to heparin salts.

Anticoagulant polymers are also of interest for drug delivery and diagnostic approaches. Here, the prevention of non-specific and immunologic interactions of the carriers (nanoparticles, micelles, vesicles etc.) with the various blood components (cells, proteins), represents an important task.

By using biocompatible, anticoagulant "stealth" polymers an improved stability and blood circulation time can be reached, promoting the diagnostic or therapeutic functions.[18]

If such anticoagulant polymers can be additionally attached to solid surfaces, the application field is further enlarged and includes the biomedically relevant area of implant material functionalization. Existing synthetic biomaterials introduced into the human body, e.g. as implantable devices, often suffer from problems associated with surface-induced thrombosis, clot formation, and infection. Implants coated with nonthrombogenic, biocompatible materials would

not only reduce the need for aggressive anticoagulant therapies, they would also be beneficial for cardiovascular applications, where the blood response to artificial materials, including thrombosis and platelet deposition, limits the long-term efficacy. The surface modification of these devices with anticoagulant polymers could increase their working life span due to an increased biocompatibility.[19]

Furthermore, zwitterionic, anticoagulant polymers are promising materials for extracorporal blood contacting applications, in particular dialysis membranes, which are massively used to separate metabolites from blood of patients with nephrologic diseases. Here the blocking of the membrane pores by blood clot formation and biofouling needs to be prevented.

A class of polymers with a high biocompatibility and antifouling properties are poly(2-oxazoline)s (POx), in particular the water soluble (co)polymers based on 2-methyl-2-oxazoline (MeOx) and 2-ethyl-2-oxazoline (EtOx).[20-28] They exhibit similar properties as poly(ethylene glycol) (PEG),[29] but have some additional advantages such as a higher stability[30, 31] and a lower viscosity.[23, 32] Although having excellent blood compatibility, there are no reports on anticoagulant POx to the best of our knowledge. In contrast, a study published recently showed that POx-based copolymers exhibit no impact on the blood clotting time.[33] However, the synthesis of POx by living cationic ring-opening polymerization (CROP) and the broad variety of functional 2-oxazoline monomers, initiators, and terminating agents, enable the preparation of tailor-made polymers, with adjustable molar masses, narrow molar mass distributions, and tunable properties.[34-39] Previously, well-defined (co)polymers based on 2-(3-butenyl)-2-oxazoline (ButEnOx)[40-42] and 2-(9-decenyl)-2-oxazoline (DecEnOx)[43-47] have been reported, which provide a platform for efficient post-polymerization modifications via thiol-ene photoaddition and, thus, enable the introduction of further functionalities.

Here we report the synthesis of zwitterionic POx and the evaluation of their blood compatibility with the focus on blood clotting. To this end, a double bond containing copolymer of ButEnOx and EtOx was prepared. Modification with 2-dimethylaminoethanethiol hydrochloride by thiole-ene addition resulted in the introduction of tertiary amine pendant groups. Subsequent functionalization with 1,3-propansultone and *β*-propiolactone yielded zwitterionic POx, a sulfobetaine POx (SB-POx) and a caboxybetaine POx (CB-POx), respectively. For comparison, a PEtOx homopolymer was prepared. All polymers were characterized by means of ^{1}H NMR spectroscopy and size exclusion chromatography (SEC). Afterwards, the influence of the polymers on the aggregation and hemolysis of erythrocytes, the whole blood viscosity, the platelet and complement activation as well as the blood coagulation was studied. Moreover, their cytotoxic activity was investigated.

Results and discussion

Synthesis of amine end-functionalized P(EtOx$_{30}$-*stat*-ButEnOx$_{10}$) and PEtOx$_{40}$

The synthesis of water-soluble zwitterionic POx was accomplished *via* the post-polymerization modification of ButEnOx-based copolymers. First, the kinetics of the copolymerization of EtOx and ButEnOx has been investigated. As already reported for the methyl triflate initiated copolymerzation at 70 °C, the methyl tosylate initiated reaction at 140 °C shows a first-order kinetic behavior (Figure S1A).[42] The observed linear increase of $\ln([M]_0/[M]_t)$ with time, demonstrates a constant concentration of propagating species indicative of a living polymerization mechanism. However, due to the higher temperature the polymerization proceeds much faster. The polymerization constants of both monomers, k_p(EtOx) = 0.206 L mol^{-1} s^{-1} and

k_p(ButEnOx) = 0.188 L mol^{-1} s^{-1}, are in the same range suggesting the formation of a random copolymer (Table S1, Figure S1A). In addition, characterization by size exclusion chromatography (SEC) showed an increasing molar mass with time and narrow molar mass distributions (Table S1, Figure S1B).

For the intended synthesis of zwitterionic POx, amine end-functionalized P(EtOx$_{30}$-*stat*-ButEnOx$_{10}$) (**2**) was prepared as a starting material in an easy, two-step procedure (Scheme 1). To this end, the living species of the CROP was quenched with potassium phthalimide. The end-capping efficiency was calculated to be 100% according to ^{1}H NMR spectroscopy (Figure S1). Subsequent hydrazinolysis yielded a terminal amine group, which can be used for further reactions, *e.g.* labeling or surface attachment. While the double bond signals at 5.87 ppm and 5.04 ppm remained unchanged, the signal of the phthalimide end-group disappeared in the ^{1}H NMR spectrum, indicating the success of the reaction (Figure S1). Characterization by SEC revealed a narrow molar mass distribution for both phthalimide and amine end-functionalized polymers (Table S1) with monomodal distributions (Figure S2). For comparison an amine end-functionalized PEtOx homopolymer with a degree of polymerization of 40 has been prepared using the same procedure.

Thiol-ene photoaddition and betainization

In the next step the double bonds of the ButEnOx units within the copolymers were functionalized with 2-dimethylaminoethanethiol hydrochloride by thiol-ene photoaddition reaction. The resulting tertiary amine group is essential for the subsequent betainization with 1,3-propansultone and *β*-propiolactone, respectively. The hydrochloride, which hampered the direct

betainization under various conditions, was neutralized by dissolving the polymer in water and adding aqueous NaOH up to a pH of 14. After removing the water, the polymer was separated from the resulting salt by extraction with chloroform. The structure of the finally obtained P(EtOx$_{30}$-*stat*-*t*AmOx$_{10}$) (**3**) resembles that of poly(DMAEMA), a well-known starting material for the synthesis of zwitterionic polymers. Characterization by ^{1}H NMR spectroscopy did not only show the success of the thiol-ene photoadditon, *i.e.* the disappearance of the double bond signals, but also a shift of the signals of the CH_3 groups of the tertiary amine and the adjacent CH_2 group to lower ppm values after treatment with aqueous NaOH (Figure 1). SEC measurements revealed an increasing molar mass after the photoaddition (Table S2).

In the last step, the zwitterionic structures were formed by reacting P(EtOx$_{30}$-*stat*-*t*AmOx$_{10}$) with 1,3-propansultone (60 °C) and *β*-propiolactone (room temperature), respectively, in acetonitril for one day. The successful quarternization of the tertiary amine group was proven by ^{1}H NMR spectroscopy (Figure 2). The signals for the methyl groups attached to the amine group were shifted to higher ppm values. Moreover, new peaks, deriving from the methylene groups between the quarternized nitrogen and the head groups of the betaines, are visible. Depending on the system, characterization by SEC showed either an increasing (solvent: DMAc + 0.21% LiCl) or a decreasing ($CHCl_3$ + TEA + *i*PrOH (94:4:2)) molar mass when compared to the PEG standards.

In vitro cytotoxicity

To prove the applicability of the prepared zwitterionic polymers for biomedical applications, the *in vitro* biocompatibility was investigated. Therefore, the cytocompatibility of the polymers was studied following a standardized protocol.

The *in vitro* cytotoxicity was evaluated on the basis of an XTT assay using mouse fibroblast L929 cells and human hepatocytes HepG2 (Figure 3A). Neither PEtOx nor the zwitterionic polymers revealed any cytotoxic effect after 24 h incubation at different concentrations (ranging from 0.1 to 10 mg mL^{-1}). A detailed live/dead microscopy study of the polymer treated cells confirmed their membrane integrity (exclusion of red fluorescent propidium iodide (PI) from cell nuclei) and their excellent viability (strong green fluorescence of fluorescein diacetate (FDA) in cytoplasm) (Figure 3B). In summary, there was no cytotoxic effect caused by the zwitterionic polymers. These results confirm the low cytotoxicities generally observed for POx-based was well as zwitterionic materials.[23, 24, 48]

Erythrocyte aggregation and hemolysis

As blood is the first contact partner within the human body during intravenous administration, the polymers were tested for their general blood compatibility.

Adverse side reactions with red blood cells were evaluated in terms of erythrocyte aggregation and hemolysis upon polymer incubation. To assess the influence of the zwitterionic polymers on the red blood cell membrane, the hemolytic activity was measured photometrically by means of hemoglobin release after potential damage of erythrocytes. The polymers were investigated at different concentrations (1, 5, and 10 mg mL^{-1}) in comparison to phosphate buffered saline (PBS) as negative and Triton-X100 as positive control. Both, the PEtOx and the zwitterionic polymers revealed a hemoglobin release below 2%, proving that they do not damage the erythrocyte membrane (Figure 4A). Furthermore, the induction of erythrocyte aggregation was investigated to assess the blood compatibility of the polymers. Formation of aggregates, which

could lead to an impeded blood flow, was analyzed by UV/Vis absorption measurements for different polymer concentrations (1, 5, and 10 mg mL^{-1}) in comparison to phosphate buffered saline (PBS) as negative and branched poly(ethylene imine) (bPEI) as positive control (Figure 4B). No cluster formation was observed photometrically in the polymer treated samples and the negative control. In contrast, the positive control clearly exhibited a cell cluster formation. These results could be confirmed microscopically (Figure 4C).

To conclude, no adverse side reactions with red blood cells, representing the major cellular compartment of the blood, were observed for the two zwitterionic polymers and the PEtOx reference polymer. On that basis, all three polymers were submitted to an even more detailed blood compatibility analysis. This included the analysis of possible impacts on undesired alterations of the blood viscosity, platelet activation, complement factor activation, and finally a detailed look at possible modulations of the coagulation pathways.[49]

Blood viscosity

Polymers entering the blood stream could possibly interfere with different blood components, such as plasma proteins and cellular membrane structures of blood cells, leading to a critical change of the whole blood viscosity. Since an appropriate blood viscosity is crucial for the proper function of blood, alterations would have a severe impact on the cardiovascular system and heart function. Measuring the blood viscosity following incubation with polymers allowed the unspecific estimation of strong mutual reactions of the polymers with whole blood components.

The whole blood viscosity was measured after the addition of the polymers in different concentrations (1, 5, and 10 mg mL^{-1}, respectively). To distinguish between a change in viscosity

caused by the intrinsic viscosity of the polymer and a polymer mediated interaction or aggregation of blood components, the viscosities of the blood/polymer solutions as well as the corresponding solutions containing only polymer (in PBS) at equivalent concentrations were compared. It turned out that the concentration dependent increase of the blood viscosity can be fully attributed to the intrinsic viscosity of the added polymer (Figure 5). As a consequence, no substantial interactions of the polymers with blood components leading to an increase or decrease of the blood viscosity were observed. The slightly increased values obtained by the addition of highly concentrated polymer solutions are in the physiological tolerable range.[50] Besides, it is rather unlikely, that a biomedically used polymer will be administered to the blood flow at such high concentrations.

Platelet activation

The activation of platelets at sites of damaged blood vessels displays a very early event in the complex process of primary hemostasis, which is finally leading to the plug like coagulation of blood via the formation of fibrin stabilized platelet aggregates. By introducing a polymeric material this sensitive system can be fatally destabilized. A malfunction of platelets could provoke excessive bleeding, whereas an exceeding platelet activity would cause spontaneous blood clot formation resulting in a life-threatening clogging of vessels.

Immunologically, platelets can be distinguished from other blood cells by the constitutive expression of the surface antigen CD42. Additionally, the CD62p (P-Selectin) membrane glycoprotein is exclusively induced on activated platelets. The latter marker was used to identify the status of activation in human platelets upon incubation with the polymers. The measurement

of the CD42/CD62p co-expression in platelet samples treated with the polymers at different concentrations (1, 5, and 10 mg mL^{-1}) and incubation times (10 and 30 min) revealed that there was no effect of the zwitterionic polymers as well as the PEtOx control polymer on the CD62p expression in CD42 positive cells. The percentage of activated platelet phenotype in terms of CD62p positive cells stayed at the constant low level of the control sample treated only with PBS.

To exclude measurement errors, platelets of the positive control were treated with thrombin, an endogenous inducer of platelet activation. Within 10 min an immediate up-regulation up to 95% of the CD62 expression was observed, indicating the sensitivity and proper setup of the assay (Figure 6).

Complement activation

A polymer introduced into the human organism is very likely to be recognized as a foreign substance by the interaction with the complement system, which plays a crucial role in the detection, opsonization and clearance of the host components, microorganisms and cells. Complement factors are a group of proteins acting in different cascade like activation pathways, including the interaction of complement factors with antibody−antigen complexes and bacterial carbohydrates as well as the binding to foreign surfaces. As a consequence, either macrophages recognize and phagocytose these elements or so called membrane attack complexes lead to a lysis of opsonized cells.[51] Even though the complement activation pathways are very complex they share the generation of the enzyme C3-convertase, which is able to activate complement component C3 creating C3b and C3a. Hence the anaphylatoxin C3a was used within a commercial immunoassay kit to detect the general activation of the complement system upon

interaction with the zwitterionic polymers.[49, 52] C3a levels were measured after incubation for 10, 30, and 60 min with different concentrations of the polymers (1, 5, and 10 mg mL^{-1}) and compared to a saline control and C3a low/high standards (Figure 7). No activation of the complement system was observed following the incubation with the zwitterionic polymers and the PEtOx control. In all cases the C3a levels remained on the level of the negative control containing only saline.

Similar results were found in a previous study analyzing the effect of zwitterioninic structures on blood compatibility issues where only a slight increase of the C3a concentration occurred compared to the negative control.[53]

Blood coagulation

The viscosity measurements of polymer treated whole blood samples already proved that there was no significant induction of blood coagulation mediated by the zwitterionic polymers. A deeper insight into possible interactions with the blood coagulation system and a possibly altered coagulation ability of the blood was gained by measuring parameters for the intrinsic (*in vivo* triggered by contact to collagen exposed in damaged tissue), extrinsic (*in vivo* activated by tissue factor released from damaged tissue), and the common coagulation pathway (conversion of fibrinogen into fibrin). The activated partial thromboplastin time (APTT) and the prothrombin time (PT) are used to examine mainly the intrinsic and extrinsic pathways, respectively. However, they both end up in the common pathway and, hence, indirectly display also the status of that pathway. In the secondary hemostasis reaction, the coagulation factors mediate the strengthening of the platelet plug formed in the primary hemostasis reaction. An aberration of the

cascade-like activation of the coagulation factors, which are mainly proteases and glycoprotein cofactors, could lead to pathology-like, uncontrolled bleeding or thromboembolism.

The PT assay revealed that an interaction of the zwitterionic polymers with the components responsible for the extrinsic blood coagulation pathway can be excluded. All obtained PT values for the polymers and the saline control were ca. 10 s, fitting into the clinically normal range of 7 to 10 s (Figure 8A). The same is valid for the PEtOx control polymer sample.

In contrast, the APTT values for the zwitterionic polymers show a clear elongation of the time, which is required to form a fibrin clot in the plasma. As measured with the Pathrombin SL activator (Figure 8B), the APTTs for the CB-POx at all concentrations were much longer than the clinical range of 26 to 42 s [206s (1 mg mL^{-1}); 220s (5 mg mL^{-1}); >>240s (10 mg mL^{-1})]. Also the SB-POx induced a retarded, but less exceeding, coagulation time depending on the used concentration [40 s (1 mg mL^{-1}); 109 s (5 mg mL^{-1}); 92 s (10 mg mL^{-1})]. Interestingly, PEtOx without zwitterionic groups showed no influence on the coagulation characteristics (all APTT around 30 s), proving its completely inert properties in this assay. These results were confirmed by using a second APTT activator (SyntASiL), known to be even more sensitive (Figure 8C).

The elongation in coagulation times, mediated by the zwitterionic polymers, indicates an anticoagulant activity via the intrinsic pathway, which is mainly consisting of the factors V, VIII, IX, X, XI, and XIII. It is very likely that the zwitterionic sulfobetaine/carboxybetaine groups interact with one or more of the downstream clotting factors, but due to the complexity, our preliminary study on the coagulation pathways does not give sufficient information to speculate on the mechanism of coagulation factor interaction with the zwitterionic polymers. Nevertheless, it is known that zwitterionic polymers based on carboxy- and sulfobetaine functionalities exhibit

anticoagulant activity, mainly attributed to the high hydrophilicity and the overall charge neutrality of the structures.[9-12, 15, 16, 53, 54]

From the methodological point of view, it might also be taken into account that the tested zwitterionic polymers interfere with the activation agents (silica particles and phospholipids), which are necessary for the induction of the coagulation *in vitro*. It is imaginable that, *e.g.*, the surface of the silica particles could be shielded by the polymers creating an interfacial hydration layer around these particles attenuating the activation reaction.

Conclusion

The blood compatibility of zwitterionic POx has been investigated with special focus on the anticoagulant activity. Therefore, a 2-oxazoline-based poly(carboxybetaine) (CB-POx) and a poly(sulfobetaine) (SB-POx) have been prepared by post-polymerization modification of P($EtOx_{30}$-*b*-$ButEnOx_{10}$). For comparison a PEtOx homopolymer with the same overall degree of polymerization (DP = 40) has been synthesized. The polymers were characterized by means of ^{1}H NMR spectroscopy and SEC, showing the suitability of the used synthesis route via thiol-ene photoaddition with a tertiary amine-containing thiol species followed by betainization. *In vitro* experiments revealed an excellent cytocompatibility of the zwitterionic POx-based polymers, since no viability reduction occurred in L929 mouse fibroblasts and human hepatocytes HepG2 after incubation with the polymers. Moreover, no adverse reactions with human blood occurred in terms of alterations of the whole blood viscosity. Also on the cellular level, no harmful effects were observed, since the zwitterionic polymers did not induce aggregation or lysis of erythrocytes and also did not lead to platelet activation. Additionally, no interference with the

immune activation via the complement system was detected. Exceedingly, an anticoagulant activity *via* the intrinsic coagulation pathway was observed for the poly(carboxybetaine)s and to a lesser extent for the poly(sulfobetaine)s.

The presented properties of the zwitterionic polymers make them promising alternatives to the widely used antithrombogenic heparin and further investigations concerning the possible mode of action and *in vivo* activity should be performed. Moreover, the zwitterionic polymers display promising candidates for blood contacting materials, such as antithrombogenic membranes (*e.g.*, for blood dialysis) and implants. In addition, their excellent biocompatibility combined with their anticoagulant activity could be useful for diagnostic and targeted delivery systems with the aim to reduce unspecific interactions with blood components and thereby increase the blood circulation time.

Experimental Section

Chemicals and Instrumentation

1,3-Propanesultone was obtained from Sigma Aldrich. Dry acetonitrile, 2-dimethylaminoethanethiol hydrochloride, β-propiolactone, EtOx, and methyl tosylate (MeOTs) were purchased from Acros Organics. ButEnOx was prepared as described earlier.[42] EtOx, ButEnOx, and MeOTs were distilled to dryness over barium oxide (BaO), and stored under nitrogen. The synthesis of P(EtOx) homopolymer is described elsewhere.[23] The amine end-functionalizatoin was performed according to the here reported procedure.

^{1}H NMR spectra were recorded on a Bruker AC 300 MHz at 298 K. Chemical shifts are reported in parts per million (ppm, δ scale) relative to the residual signal of the deuterated solvent.

Size exclusion chromatography (SEC) investigations of the polymers were measured on two systems: 1) An Agilent Technologies 1200 Series gel permeation chromatography system equipped with a G1329A autosampler, a G131A isocratic pump, a G1362A refractive index detector, and both a PSS Gram 30 and a PSS Gram 1000 column placed in series. As eluent a 0.21% LiCl solution in *N,N*-dimethylacetamide (DMAc) was used at 1 mL min^{-1} flow rate and a column oven temperature of 40 °C. 2) A Shimadzu system equipped with a SCL-10A VP system controller, a DGU-14A degasser, a LC-10AD VP pump, a RID-10A refractive index detector and a PSS SDV column running with chloroform, triethylamine (TEA), and 2-propanol (94 : 4 : 2) as eluent. The Techlab column oven was set to 50 °C. For both systems, molar masses were calculated against poly(styrene) standards.

For the photometric absorbance measurement, a TECAN Infinite M200 PRO plate reader (TECAN, Crailsheim, Germany) was used to measure the absorption of samples from (a) the XTT cytotoxicity assay (570 nm with a background correction of the optical density (OD) at 690 nm), (b) the hemolysis of erythrocytes (540 nm with a background correction of the OD at 690 nm), (c) the photometric evaluation of erythrocyte aggregation (645 nm), and (d) the activation of complement factors C3a and SC5b-9 (450 nm). Each well containing the sample was measured in four different spots each with 10-25 flashes per scan. The evaluation of platelet activation was performed by flow cytometry (FC) measured on a Beckmann Coulter Cytomics FC-500 equipped with Uniphase Argon ion laser, 488 nm, 20 mW output and analyzed with the Cytomics CXP software. The blood coagulation time was spectroscopically determined with the clinical coagulation analyzer BCS XP 1.1 (Siemens Healthcare Diagnostics, Marburg, Germany). Viscosity measurements were conducted on an AMVn rolling ball viscometer (Anton Paar, Graz, Austria) and the density of the solutions was measured by a densitometer (DMA 4100, Anton Paar, Graz, Austria). To visualize the viability of cells after incubation with the polymers, the

blue/red/green fluorescence signal of cells cultured in a 96 well plate and stained with Hoechst 33342/ fluorescein diacetate (FDA)/propidium iodide (PI) was observed on a fluorescence microscope (Cell Observer Z1, Carl Zeiss, Jena, Germany) equipped with a mercury arc UV lamp and the appropriate filter combinations for excitation and detection of emission. Images of a series were captured with a 10 objective using identical instrument settings (e.g. UV lamp power).

Erythrocyte aggregation was observed microscopically using an inverse light microscope (Zeiss AX 10 Vert A1, 100 and 400 × magnification).

Synthesis of phthalimide end-capped P(EtOx$_{30}$-*stat*-ButEnOx$_{10}$) (1)

A solution of initiator (MeOTs), solvent (acetonitrile), and monomers (EtOx, ButEnOx) was prepared with a [EtOx]/[ButEnOx]/[I] ratio of 30:10:1. The total monomer concentration was adjusted to 3 M. The solution was heated at 140 °C in a microwave synthesizer for a predetermined time and subsequently cooled to room temperature. A 2-fold excess of potassium phthalimide was added and the reaction mixture was stirred at 70 °C overnight. After filtration, the solvent was removed. The residue was dissolved in dichloromethane and washed with water, a saturated aqueous solution of $NaHCO_3$, and brine. The organic phase was dried over sodium sulfate, filtered, and concentrated. After precipitation into ice-cold diethyl ether, the polymer was dried at 40 °C.

Synthesis of amine end-functionalized P($EtOx_{30}$-*stat*-$ButEnOx_{10}$) (2)

Phthalimide end-capped P($EtOx_{30}$-*stat*-$ButEnOx_{10}$) was dissolved in ethanol and refluxed overnight with a 10-fold excess of hydrazine monohydrate. After cooling to room temperature, the pH was adjusted to 2-3 using concentrated HCl. The precipitate filtered off and the ethanol was evaporated. After dissolving the residue in water, aqueous NaOH was added up to pH 9 to 10. The aqueous phase was extracted thrice with chloroform. The combined organic layers were dried over sodium sulfate, concentrated, and precipitated into ice-cold diethyl ether. The white precipitate was filtered off and dried at 40 °C under reduced pressure.

Functionalization with 2-dimethylaminoethanethiol hydrochloride (3)

A 5% solution of P($EtOx_{30}$-*stat*-$ButEnOx_{10}$), 0.1 mol% 2,2-dimethoxy-2-phenylacetophenone (DMPA) per double bond, and a 2-fold excess per double bond of 2-dimethylaminoethanethiol hydrochloride in methanol was degassed with nitrogen for 30 min. Subsequently, the reaction mixture was stirred in a UV chamber (λ = 365 nm) overnight. The solvent was evaporated. The polymer was dissolved in water and aqueous NaOH was added up to pH 14. After evaporation of the water, chloroform was added and the salt removed by filtration. The organic phase was dried over sodium sulfate, filtered, concentrated under reduced pressure, and precipitated into ice-cold diethyl ether. The product was dried under reduced pressure at 40 °C for three days.

Betainization with 1,3-propanesultone (4)

To a 5% solution of P($EtOx_{30}$-*stat*-*t*$AmOx_{10}$) in dry acetonitrile a 2-fold excess of 1,3-propanesultone per tertiary amine group was added. The reaction mixture was stirred at 60 °C

overnight. Subsequently, the solvent was concentrated and the polymer precipitated into ice-cold diethyl ether. The product was dried under reduced pressure at 40 °C for three days. At last, the product was dissolved in a small amount of water and lyophilized.

Betainization with *β*-propiolactone (5)

To a 4.5% solution of P($EtOx_{30}$-*stat*-*t*$AmOx_{10}$) in dry acetonitrile a 1.1-fold excess of 1,3-propanesultone per tertiary amine group was added. The reaction mixture was stirred at room temperature for one day. After evaporation of the solvent, the polymer was purified by preparative size exclusion chromatography (Sephadex® SX-1, solvent: dichloromethane). The product was dried under reduced pressure at 40 °C for three days. At last, the product was dissolved in a small amount of water and lyophilized.

Polymer cytotoxicity

For the cytotoxicity experiments, the mouse fibroblast cell line L929 and the human hepatocyte cell line HepG2 were purchased from a commercial cell bank (Cell line service, Eppelheim, Germany). The cells were routinely cultured as follows: Cell culture media [Dulbecco's modified eagle's medium (DMEM) for L929 cells and DMEM/F-12 for HepG2 cells] were supplemented with 10% fetal calf serum, 100 U mL^{-1} penicillin, and 100 µg mL^{-1} streptomycin (all components from Biochrom, Berlin, Germany) at 37 °C in a humidified atmosphere with 5% (v/v) CO_2. The cytotoxicity was determined with a XTT assay following the ISO/EN 10993 part 5 protocol: Cells (L929 and HepG2) were seeded in 96-well plates at a density of 1×10^4 cells/well and grown as monolayer cultures for 24 h. The cells were then incubated separately with different

polymer concentrations (from 0.01 to 10.00 mg mL^{-1} (n = 6)) for 24 h. Control cells were incubated with fresh culture medium. After incubation, 50 µL of a XTT solution prepared according to the manufacturer's instructions were added to each well. After 4 h at 37 °C, 100 µL of each solution were transferred to a new microtiter plate and the optical density (OD) was measured photometrically. The negative control was standardized as 0% of metabolism inhibition and referred as 100% viability. Experiments were run in sextuplicate.

In addition, the viability of the cells after exposure to the polymers was examined microscopically using a modified fluorescein diacetate (FDA)/propidium iodide (PI) viability assay.[55]

Hemolysis of erythrocytes

For testing the hemolytic activity of the polymer solutions, blood from three unmedicated and healthy donors was collected (Institute for Transfusion Medicine, Friedrich Schiller University Jena) and stabilized by sodium citrate. After centrifugation at 4.500 × g for 5 min, the pellet was washed three times with cold 1.5 mM phosphate buffered saline pH 7.4 (PBS). After dilution with PBS in a ratio of 1:7 (number of erythrocytes approx. 2×10^6 mL^{-1}), aliquots of the erythrocyte suspension were mixed 1:1 with the polymer solutions (final polymer concentrations in the erythrocyte suspension of 10 mg mL^{-1}, 5 mg mL^{-1} and 1 mg mL^{-1}) and incubated in a water bath at 37 °C for 60 min. After centrifugation at 2400 g for 5 min the hemoglobin release into the supernatant was determined spectrophotometrically using a microplate reader at 544 nm wavelength. Complete hemolysis was achieved using 1% Triton X-100 reflecting the 100% value. PBS served as negative control. Less than 5% hemolysis rate were taken as non-hemolytic. Experiments were run in triplicate and were repeated once.

Erythrocyte aggregation

Erythrocyte aggregation induced by the polymers were tested using a photometric and microscopic method according to literature.[56] Erythrocytes were isolated as described above. Erythrocyte suspensions (100 µL) containing 2 Mio erythrocytes per mL were mixed with the same volume of polymer solutions (20, 10 and 2 mg mL-1 diluted in PBS buffer) in a clear flat bottomed 96-well plate. The cells were incubated under vigorous shaking at 37 °C for 2 h, and the absorbance was measured at 645 nm in a microplate reader. 25 kDa bPEI (50 µg/mL) was used as positive control. As negative controls, cells were only treated with PBS. Blank values were determined with PBS and subtracted from the sample values. Absorbance values of the test solutions lower than the negative control were regarded as aggregation. Experiments were run in triplicate and were repeated once.

Additionally, erythrocyte aggregation was evaluated by microscopic observations using 10 × diluted samples from the above described photometric determinations.

Blood viscosity

The influence of the polymers on blood viscosity was tested according to a formerly published setup.[33] The pooled blood of three unmedicated and healthy donors was collected (Institute for Transfusion Medicine, Friedrich Schiller University Jena) and stabilized by sodium citrate. Within 4 hours after collection, 200 µL of PBS or polymer solution (50 mg mL^{-1}, 10 mg mL^{-1} and 5 mg mL^{-1} to obtain final polymer concentrations in the whole blood of 10 mg mL^{-1}, 5 mg mL^{-1} and 1 mg mL^{-1}) were added to 800 µL of whole blood and incubated for 30 min at 37 °C. In a parallel setup, PBS was used instead of the whole blood sample to measure the dynamic viscosity

of PBS and the corresponding polymer solutions. Viscosity measurements were conducted at 20 °C using an AMVn (Anton Paar, Graz, Austria) rolling ball viscometer at three inclination angles (50°/70°/85°) of the capillary. For normalization, the dynamic viscosity values of the polymers diluted in whole blood or phosphate buffered saline were divided by the viscosity value of the pure blood or PBS, respectively, and results are expressed as relative dynamic viscosity.

Platelet activation

The blood of three unmedicated and healthy donors was collected (Institute for Transfusion medicine, Friedrich Schiller University Jena) and stabilized by sodium citrate. The platelet rich plasma (PRP) was isolated by centrifugation, pooled, and used immediately. To 240 µL of PRP 60 µL of PBS or polymer solution (50 mg mL^{-1}, 10 mg mL^{-1} and 5 mg mL^{-1} to obtain final polymer concentrations in the PRP of 10 mg mL^{-1}, 5 mg mL^{-1} and 1 mg mL^{-1}) were added and incubated for 10 min or 30 min at 37 °C. To activate platelets 0.5 U mL^{-1} of bovine thrombin (Sigma, Taufkirchen, Germany) were added to the positive control instead of the polymer solution. Aliquots containing 50 µL of the incubated mixture were removed and fixed for 10 min at room temperature using 4% paraformaldehyde in PBS. After washing and centrifugation a double immuno-staining was performed using 20 µL of FITC labeled monoclonal antibody directed against CD42 and 20 µL of phycoerythrin (PE) labeled monoclonal antibody directed against CD62P. Isotype controls were incubated with mouse IgG antibodies conjugated with fluorescein isothiocyanate (FITC) or PE dye, respectively (all antibodies were purchased from BD Biosciences, Heidelberg, Germany). After 30 min incubation at room temperature the activation state of the platelets was determined using fluorescence flow cytometry. Expression of the platelet activation marker CD62P and the constitutively present platelet marker CD42 were

detected using a Beckmann Coulter Cytomics FC-500 equipped with Uniphase Argon ion laser, 488 nm, 20 mW output. Overall 100.000 platelets were measured per sample and analyzed with the Cytomics CXP software. The experiment was repeated three times.

Complement activation

The complement activation was measured on the basis of C3a anaphylatoxins with the appropriate ELISA kit (Quidel, San Diego, USA). The blood of three unmedicated and healthy donors was collected (Institute for Transfusion Medicine, Friedrich Schiller University Jena) and stabilized by sodium citrate. The plasma was isolated by centrifugation, pooled, and used immediately. 40 µL of plasma were mixed with 10 µL PBS or polymer solution (50 mg mL^{-1}, 10 mg mL^{-1} and 5 mg mL^{-1} to obtain final polymer concentrations in the plasma of 10 mg mL^{-1}, 5 mg mL^{-1} and 1 mg mL^{-1}) and incubated for 10, 30, and 60 min. Subsequently, samples, standards, and controls were diluted in the ratio 1:200 with sample buffer provided by the supplier and applied to a 96 well plate pre-coated with an antibody directed against C3a epitopes. Further incubation steps were performed according to the instructions of the supplier. The C3a concentrations were measured as absorption (at 450 nm) of the chromogenic substrate added during performance of the assay. Experiments were run in triplicate.

Blood coagulation

The blood of three unmedicated and healthy donors was collected (Institute for Transfusion Medicine, Friedrich Schiller University Jena) and stabilized by sodium citrate. The plasma was isolated by centrifugation at 4000 g for 3 min at room temperature and used within 3 hours. The

prothrombin time (PT) and the activated partial thromboplastin time (APTT) were spectroscopically determined with the clinical coagulation analyzer BCS XP 1.1 (Siemens Healthcare Diagnostics, Marburg, Germany). To 240 µL of plasma 60 µL of PBS or polymer solution (50 mg mL^{-1}, 10 mg mL^{-1} and 5 mg mL^{-1} to obtain final polymer concentrations in the plasma of 10 mg mL^{-1}, 5 mg mL^{-1} and 1 mg mL^{-1}) were added and incubated for 5 min. Experiments were run in triplicate. For the APTT determination, the intrinsic and common coagulation pathways were activated by adding 100 µL Pathrombin SL activator (Siemens Healthcare Diagnostics, Marburg, Germany) to 100 µL of the probe. After 2 min incubation at 37 °C, the coagulation was triggered by calcium chloride addition (100 µL, 0.025 M) and followed spectroscopically for up to 240 s at 671 nm. Additional samples were treated identically but with 100 µL of SyntASiL activator (Instrumentation Laboratory, Kirchheim, Germany) instead of Pathrombin SL activator. The PT was determined by addition of 100 µL of Dade Innovin activator (Siemens Healthcare Diagnostics, Marburg, Germany) to 50 µL of the plasma-polymer. The coagulation reaction was followed spectroscopically for 120 s at 671 nm. Each experiment was repeated three times.

Acknowledgement

The authors want to thank the Dutch Polymer Institute (DPI, Technology Area HTE). LT wants to thank Cornelia Bader for large-scale synthesis of ButEnOx monomer. KK is grateful to the Alexander von Humboldt foundation for financial support.

References

1. H.-W. Chien, C.-C. Tsai, W.-B. Tsai, M.-J. Wang, W.-H. Kuo, T.-C. Wei and S.-T. Huang, *Colloids and Surfaces B: Biointerfaces*, 2013, **107**, 152-159.
2. N. Y. Kostina, C. Rodriguez-Emmenegger, M. Houska, E. Brynda and J. Michálek, *Biomacromolecules*, 2012, **13**, 4164-4170.
3. Z. Zhang, T. Chao, S. Chen and S. Jiang, *Langmuir*, 2006, **22**, 10072-10077.
4. Z. Zhang, J. A. Finlay, L. Wang, Y. Gao, J. A. Callow, M. E. Callow and S. Jiang, *Langmuir*, 2009, **25**, 13516-13521.
5. A. Lewis, Y. Tang, S. Brocchini, J.-w. Choi and A. Godwin, *Bioconjugate Chem.*, 2008, **19**, 2144-2155.
6. Y. Asanuma, Y. Inoue, S.-i. Yusa and K. Ishihara, *Colloids Surf., B*, 2013, **108**, 239-245.
7. T. Goda and K. Ishihara, *Expert Rev. Med. Devices*, 2006, **3**, 167-174.
8. T. Shimizu, T. Goda, N. Minoura, M. Takai and K. Ishihara, *Biomaterials*, 2010, **31**, 3274-3280.
9. W.-H. Kuo, M.-J. Wang, H.-W. Chien, T.-C. Wei, C. Lee and W.-B. Tsai, *Biomacromolecules*, 2011, **12**, 4348-4356.
10. C. Rodriguez Emmenegger, E. Brynda, T. Riedel, Z. Sedlakova, M. Houska and A. B. Alles, *Langmuir*, 2009, **25**, 6328-6333.
11. Y.-J. Shih and Y. Chang, *Langmuir*, 2010, **26**, 17286-17294.
12. Y.-J. Shih, Y. Chang, A. Deratani and D. Quemener, *Biomacromolecules*, 2012, **13**, 2849-2858.
13. H.-S. Han, J. D. Martin, J. Lee, D. K. Harris, D. Fukumura, R. K. Jain and M. Bawendi, *Angew. Chem. Int. Ed.*, 2013, **52**, 1414-1419.
14. J.-T. Sun, Z.-Q. Yu, C.-Y. Hong and C.-Y. Pan, *Macromol. Rapid Commun.*, 2012, **33**, 811-818.
15. J. Cao, Y.-W. Chen, X. Wang and X.-L. Luo, *J. Biomed. Mater. Res., Part A*, 2011, **97A**, 472-479.
16. Y. Chang, W.-Y. Chen, W. Yandi, Y.-J. Shih, W.-L. Chu, Y.-L. Liu, C.-W. Chu, R.-C. Ruaan and A. Higuchi, *Biomacromolecules*, 2009, **10**, 2092-2100.
17. Y. I. Oh, G. J. Sheng, S.-K. Chang and L. C. Hsieh-Wilson, *Angew. Chem. Int. Ed.*, 2013, **52**, 11796-11799.

18. Z. Cao and S. Jiang, *Nano Today*, 2012, **7**, 404-413.
19. A. G. Kidane, H. Salacinski, A. Tiwari, K. R. Bruckdorfer and A. M. Seifalian, *Biomacromolecules*, 2004, **5**, 798-813.
20. N. Adams and U. S. Schubert, *Adv. Drug Deliv. Rev.*, 2007, **59**, 1504-1520.
21. R. Luxenhofer, Y. Han, A. Schulz, J. Tong, Z. He, A. V. Kabanov and R. Jordan, *Macromol. Rapid Commun.*, 2012, **33**, 1613-1631.
22. H. Schlaad, C. Diehl, A. Gress, M. Meyer, A. L. Demirel, Y. Nur and A. Bertin, *Macromol. Rapid Commun.*, 2010, **31**, 511-525.
23. M. Bauer, C. Lautenschlaeger, K. Kempe, L. Tauhardt, U. S. Schubert and D. Fischer, *Macromol. Biosci.*, 2012, **12**, 986-998.
24. M. Bauer, S. Schroeder, L. Tauhardt, K. Kempe, U. S. Schubert and D. Fischer, *J. Polym. Sci., Part A: Polym. Chem.*, 2013, **51**, 1816–1821.
25. L. Tauhardt, K. Kempe, M. Gottschaldt and U. S. Schubert, *Chem. Soc. Rev.*, 2013, **42**, 7998-8011.
26. J. Kronek, J. Lustoň, Z. Kroneková, E. Paulovičová, P. Farkaš, N. Petrenčíková, L. Paulovičová and I. Janigová, *J. Mater. Sci.: Mater. Med.*, 2010, **21**, 879-886.
27. J. Kronek, E. Paulovičová, L. Paulovičová, Z. Kroneková and J. Lustoň, *J. Mater. Sci.: Mater. Med.*, 2012, **23**, 1457-1464.
28. V. R. de la Rosa, *J. Mater. Sci.: Mater. Med.*, 2013, DOI: 10.1007/s10856-013-5034-y.
29. K. Knop, R. Hoogenboom, D. Fischer and U. S. Schubert, *Angew. Chem. Int. Ed.*, 2010, **49**, 6288-6308.
30. R. Konradi, C. Acikgoz and M. Textor, *Macromol. Rapid Commun.*, 2012, **33**, 1663-1676.
31. B. Pidhatika, M. Rodenstein, Y. Chen, E. Rakhmatullina, A. Muhlebach, C. Acikgoz, M. Textor and R. Konradi, *Biointerphases*, 2012, **7**, 1-15.
32. T. X. Viegas, M. D. Bentley, J. M. Harris, Z. Fang, K. Yoon, B. Dizman, R. Weimer, A. Mero, G. Pasut and F. M. Veronese, *Bioconjugate Chem.*, 2011, **22**, 976-986.
33. K. Knop, D. Pretzel, A. Urbanek, T. Rudolph, D. H. Scharf, A. Schallon, M. Wagner, S. Schubert, M. Kiehntopf, A. A. Brakhage, F. H. Schacher and U. S. Schubert, *Biomacromolecules*, 2013, **14**, 2536-2548.
34. R. Hoogenboom, *Angew. Chem. Int. Ed.*, 2009, **48**, 7978-7994.
35. A. Makino and S. Kobayashi, *J. Polym. Sci., Part A: Polym. Chem.*, 2010, **48**, 1251-1270.

36. O. Sedlacek, B. D. Monnery, S. K. Filippov, R. Hoogenboom and M. Hruby, *Macromol. Rapid Commun.*, 2012, **33**, 1648-1662.
37. B. Guillerm, S. Monge, V. Lapinte and J.-J. Robin, *Macromol. Rapid Commun.*, 2012, **33**, 1600-1612.
38. K. Aoi and M. Okada, *Prog. Polym. Sci.*, 1996, **21**, 151-208.
39. E. Rossegger, V. Schenk and F. Wiesbrock, *Polymers*, 2013, **5**, 956-1011.
40. C. Diehl and H. Schlaad, *Macromol. Biosci.*, 2009, **9**, 157-161.
41. C. Diehl and H. Schlaad, *Chem. Eur. J.*, 2009, **15**, 11469-11472.
42. A. Gress, A. Völkel and H. Schlaad, *Macromolecules*, 2007, **40**, 7928-7933.
43. T. R. Dargaville, R. Forster, B. L. Farrugia, K. Kempe, L. Voorhaar, U. S. Schubert and R. Hoogenboom, *Macromol. Rapid Commun.*, 2012, **33**, 1695-1700.
44. B. L. Farrugia, K. Kempe, U. S. Schubert, R. Hoogenboom and T. R. Dargaville, *Biomacromolecules*, 2013, **14**, 2724-2732.
45. K. Kempe, R. Hoogenboom, M. Jaeger and U. S. Schubert, *Macromolecules*, 2011, **44**, 6424-6432.
46. K. Kempe, R. Hoogenboom and U. S. Schubert, *Macromol. Rapid Commun.*, 2011, **32**, 1484-1489.
47. K. Kempe, A. Vollrath, H. W. Schaefer, T. G. Poehlmann, C. Biskup, R. Hoogenboom, S. Hornig and U. S. Schubert, *Macromol. Rapid Commun.*, 2010, **31**, 1869-1873.
48. J. Kronek, Z. Kroneková, J. Lustoň, E. Paulovičová, L. Paulovičová and B. Mendrek, *J. Mater. Sci.: Mater. Med.*, 2011, **22**, 1725-1734.
49. R. K. Kainthan, S. R. Hester, E. Levin, D. V. Devine and D. E. Brooks, *Biomaterials*, 2007, **28**, 4581-4590.
50. C. Lenz, A. Rebel, K. F. Waschke, R. C. Koehler and T. Frietsch, *Transfus. Altern. Transfus. Med.*, 2008, **9**, 265-272.
51. C. A. Janeway, P. Travers and M. Walport, in *Immunobiology: The Immune System in Health and Disease*, Garland Science, New York, 5th edn., 2001.
52. R. K. Kainthan, J. Janzen, E. Levin, D. V. Devine and D. E. Brooks, *Biomacromolecules*, 2006, **7**, 703-709.
53. X. Wang, X. Chen, L. Xing, C. Mao, H. Yu and J. Shen, *J. Mater. Chem. B*, 2013, **1**, 5036-5044.

54. S.-H. Chen, Y. Chang, K.-R. Lee, T.-C. Wei, A. Higuchi, F.-M. Ho, C.-C. Tsou, H.-T. Ho and J.-Y. Lai, *Langmuir*, 2012, **28**, 17733-17742.

55. H. Ahrem, D. Pretzel, M. Endres, D. Conrad, J. Courseau, H. Müller, R. Jaeger, C. Kaps, D. O. Klemm and R. W. Kinne, *Acta Biomater.*, 2014, **10**, 1341-1353.

56. A. Vollrath, D. Pretzel, C. Pietsch, I. Perevyazko, S. Schubert, G. M. Pavlov and U. S. Schubert, *Macromol. Rapid Commun.*, 2012, **33**, 1791-1797.

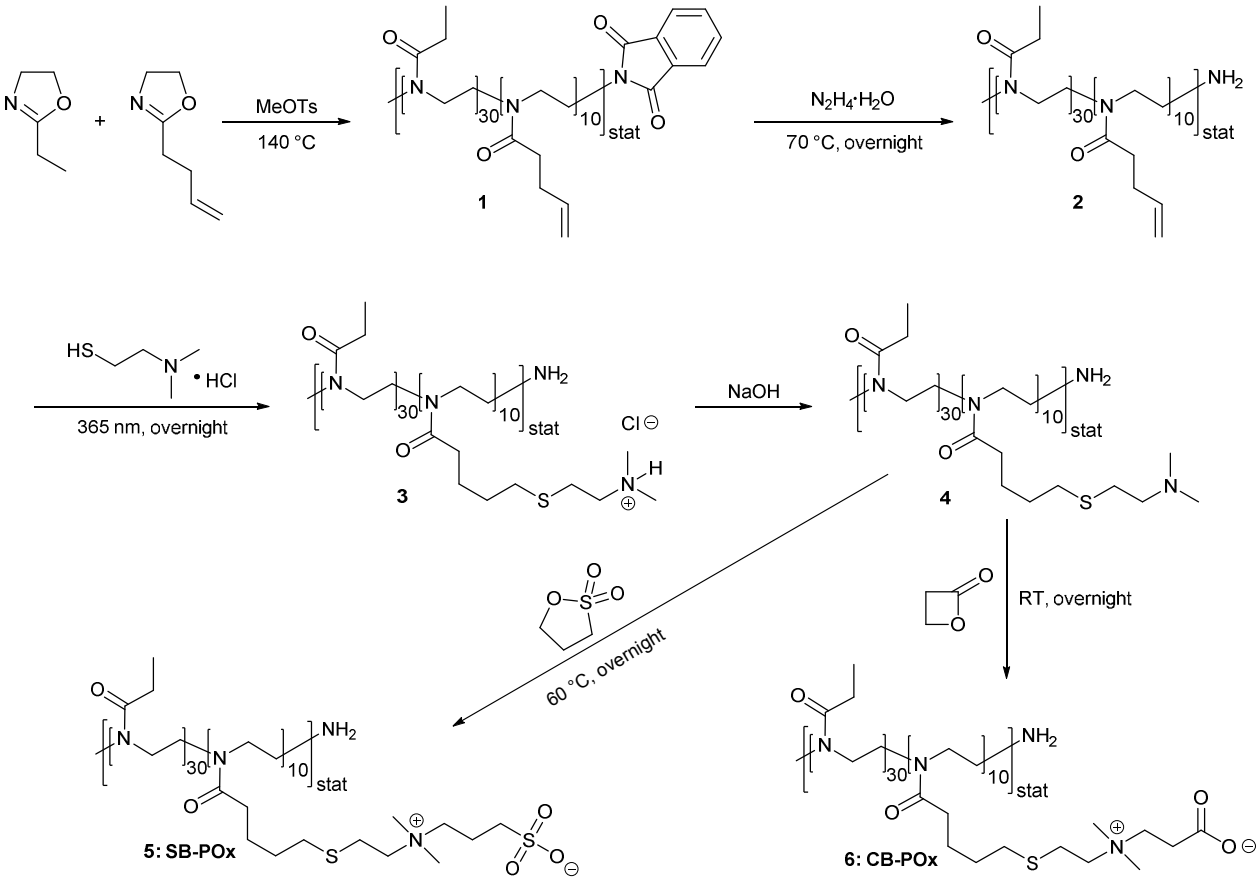

Scheme 1. Schematic representation of the synthesis of zwitterionic POx.

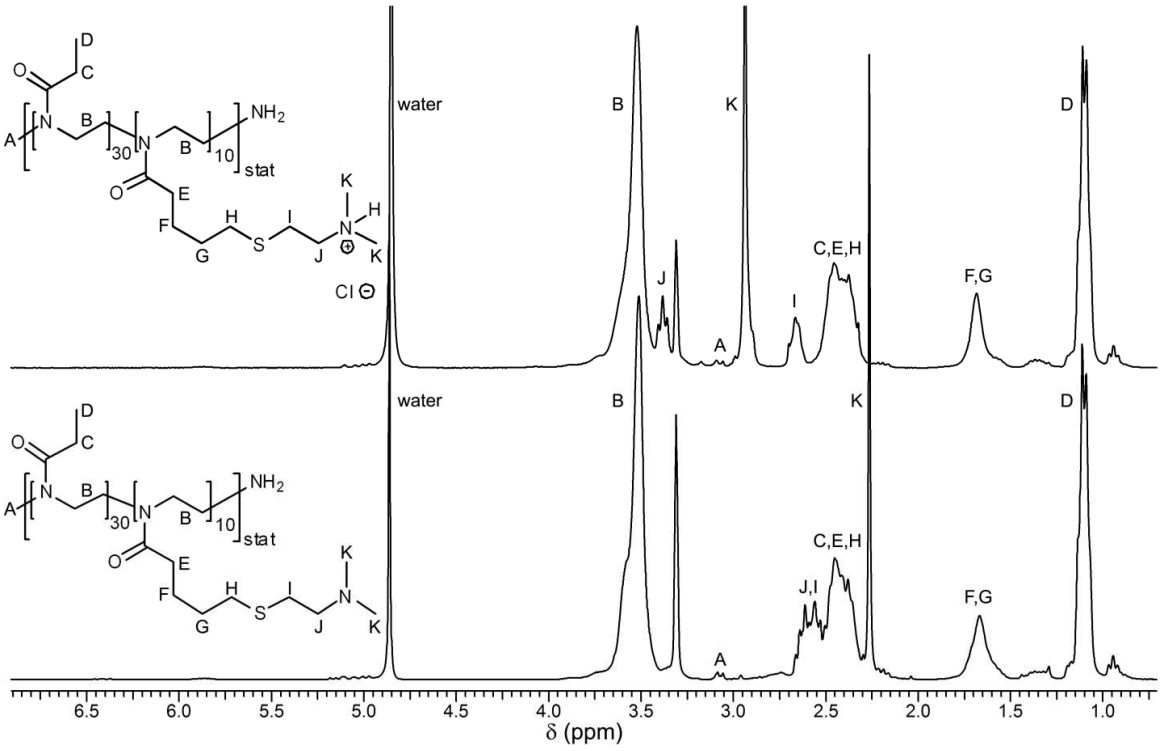

Figure 1. ^{1}H NMR spectra of P(EtOx$_{30}$-*stat*-*t*AmOx$_{10}$) (top) before and (bottom) after treatment with aqueous NaOH (300 MHz, CD_3OD).

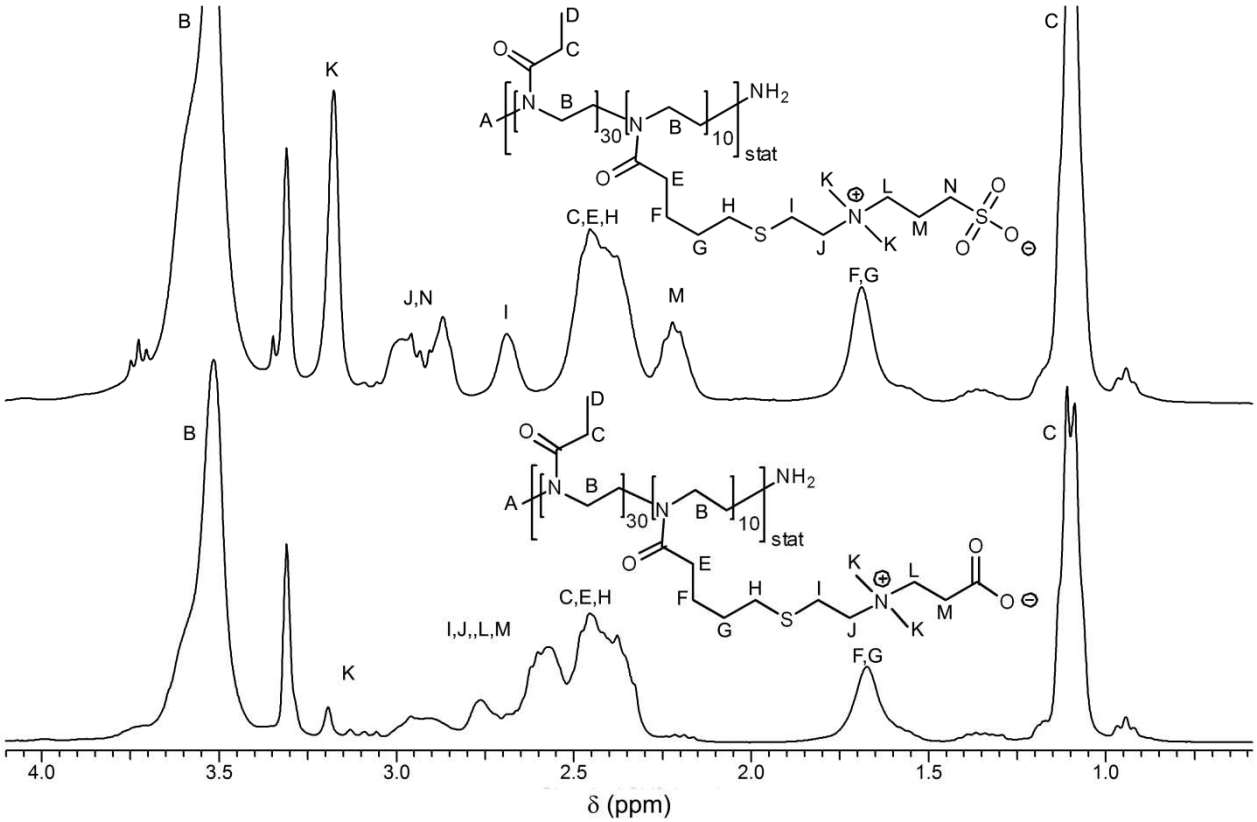

Figure 2. ^{1}H NMR spectra of the POx-based (top) poly(sulfobetaine) and (bottom) poly(carboxybetaine) (300 MHz, CD_3OD).

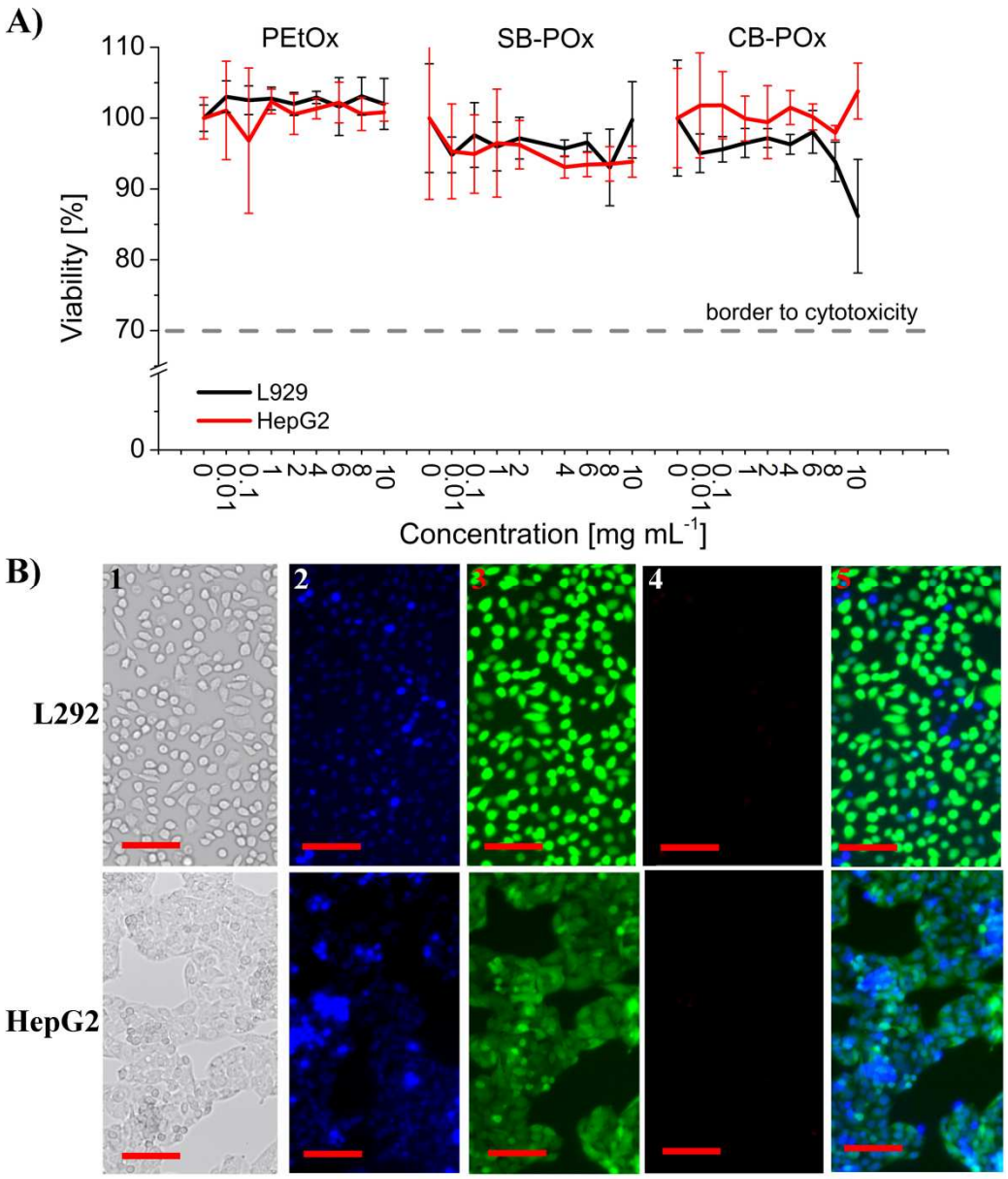

Figure 3. A) Cell viability of L929 mouse fibroblasts and human hepatocytes HepG2 after incubation with zwitterionic polymers up to 10 mg mL^{-1} for 24 hours. Cells incubated with polymer free culture medium served as control. The cell viability was determined by XTT assay according to ISO 10993-5. Data are expressed as mean ± SD of six determinations. B) Representative bright field and fluorescence micrographs of Hoechst 33342/FDA/PI stained L929 mouse fibroblast cells (upper panel) and human hepatocytes HepG2 (lower panel) cultured for 24 hours in the presence of 10 mg mL^{-1} of CB-POx (identical results for SB-POx and PEtOx). (1) Light field image, (2) blue fluorescent Hoechst 33342 dye labels nuclei of all cells present, (3) green fluorescent FDA dye indicates cytoplasm of vital cells, (4) red fluorescent PI signals tag nuclei of dead cells, and (5) overlay of Hoechst 33342 dye fluorescence and green fluorescence of the FDA dye.

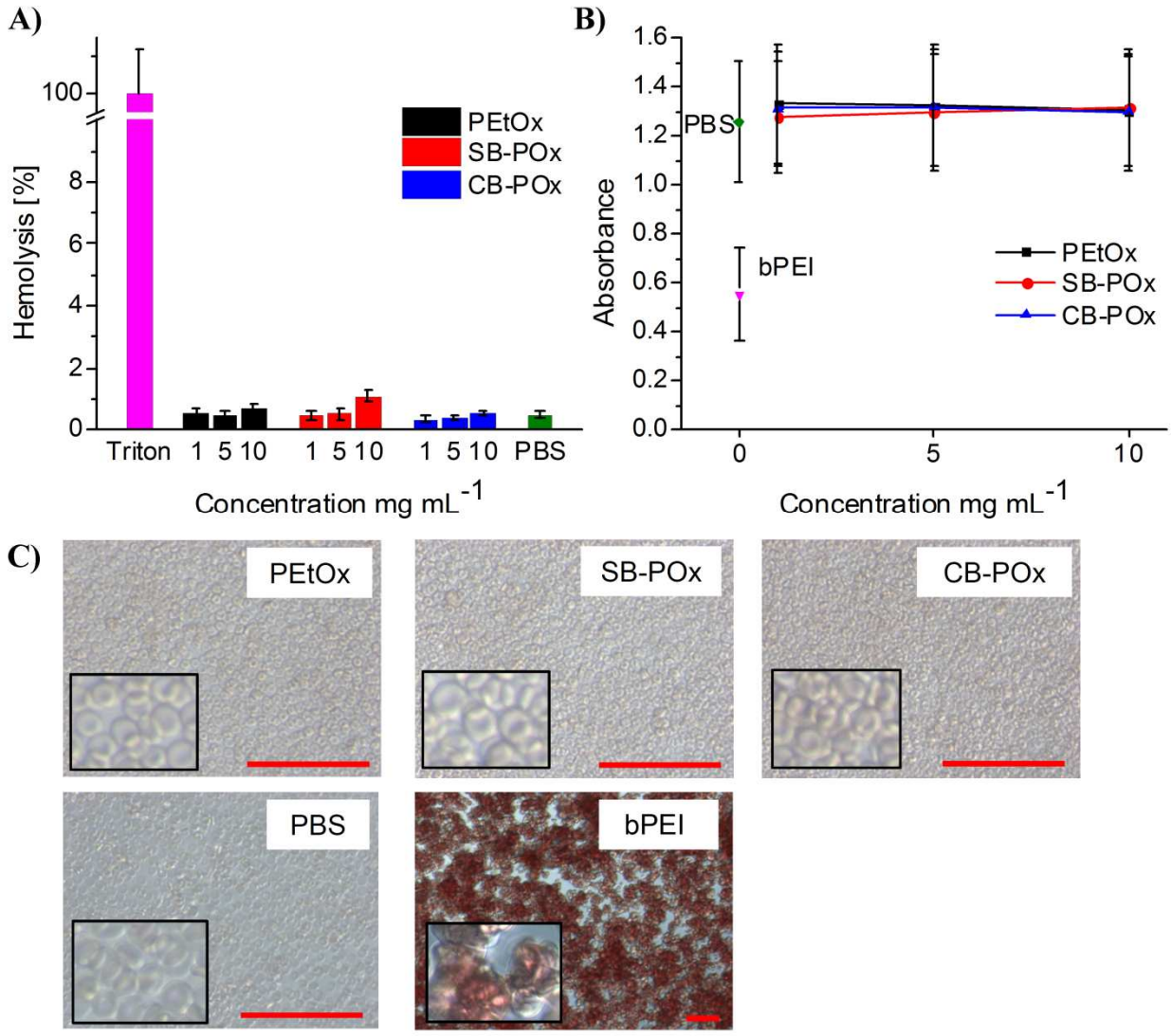

Figure 4. Blood compatibility of PEtOx and zwitterionic POx-based polymers. A) Photometric determination of hemolytic activity after incubation with different polymer concentrations for 1 h at 37 °C. Triton X-100 (1%) served as positive and PBS as negative control. Experiments were run in triplicate and were repeated once; data are presented as the mean percentage ± SD of hemolytic activity compared to the positive control set as 100%. B) Photometric determination of the erythrocyte aggregation after 2 h incubation at 37 °C with polymers. 25 kDa bPEI (50 µg mL^{-1}) served as positive and PBS as negative control. Experiments were run in triplicate and were repeated once; data are presented as the mean measured absorbance ± SD. C) Representative micrographs of red blood cell aggregation after 2 h incubation at 37 °C with polymers. PBS served as negative and 25 kDa bPEI (50 µg mL^{-1}) as positive control.

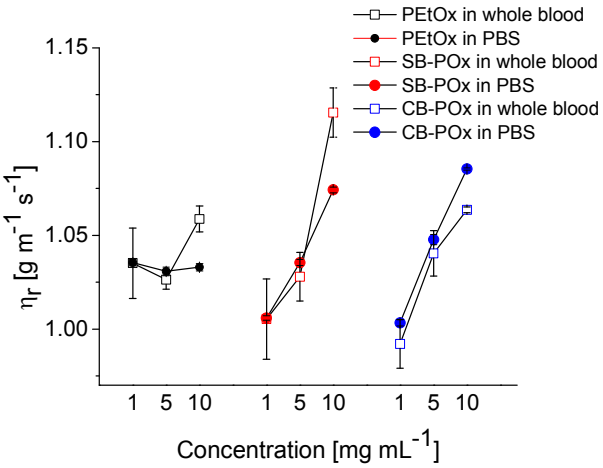

Figure 5. Blood compatibility of PEtOx and zwitterionic POx-based polymers concerning their influence on the whole blood viscosity: Relative viscosity of the polymer solutions in PBS and in whole blood. Experiments were run in quadruplicate at three inclination angles, data are presented as the mean percentage ± SD.

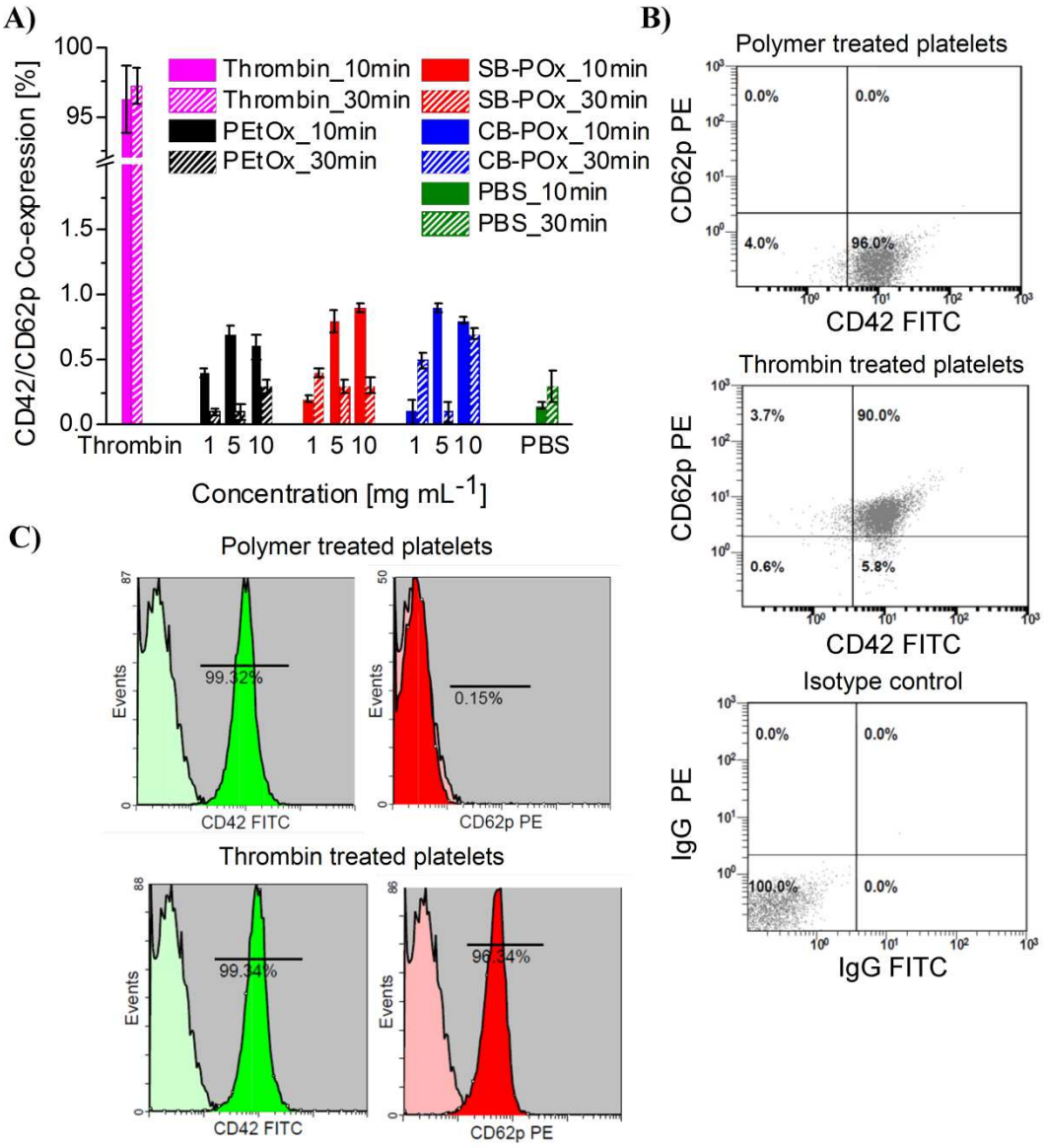

Figure 6. A) FACS analysis of polymer mediated platelet activation measured by determination of CD62p/CD42 co-expression after 10 min incubation. Experiments were run in triplicate, data are presented as percentage of platelets positive for both CD62p and CD42 epitopes ± SD. B) Representative dot-plots for the expression of CD62p and CD42 of a CB-POx treated sample and a thrombin treated positive control after 10 min incubation and, additionally, staining pattern of the isotype control. Non activated cells are in the lower right panel and only positive for CD42, cells in the upper right panel of the dot plot diagrams are double positive for CD62p and CD42, indicating an activated platelet phenotype. The absence of non-specific binding of the antibodies is proven by the very low fluorescence signal of the platelets in the isotype control, where all cells are located in the lower left panel. C) Histogram plots. The faint colored graphs indicate the value of the isotype control and green/red graph of the sample stained with the specific CD42 and CD62p antibodies.

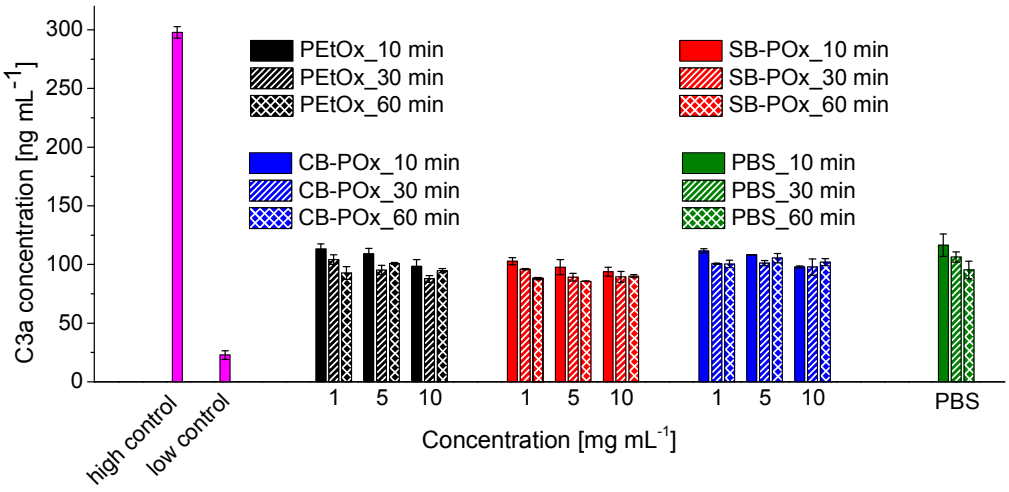

Figure 7. Complement activation by the polymers measured by determination of C3a levels after 10 min, 30 min, and 60 min incubation. Experiments were run in triplicate and data are presented as the mean measured absorbance ± SD of three determinations

A)

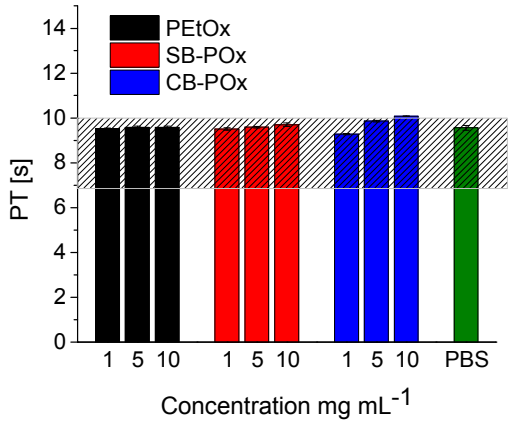

B) Pathrombin SL activator

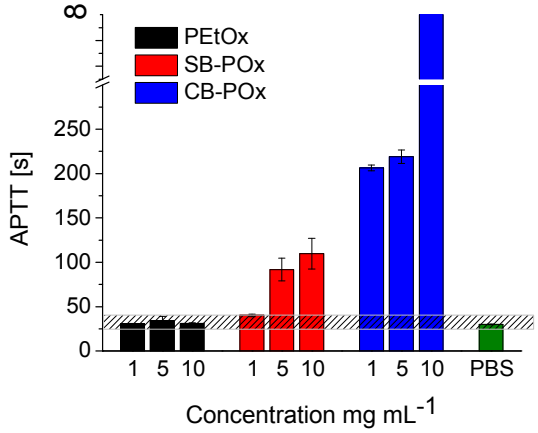

C) SyntASiL activator

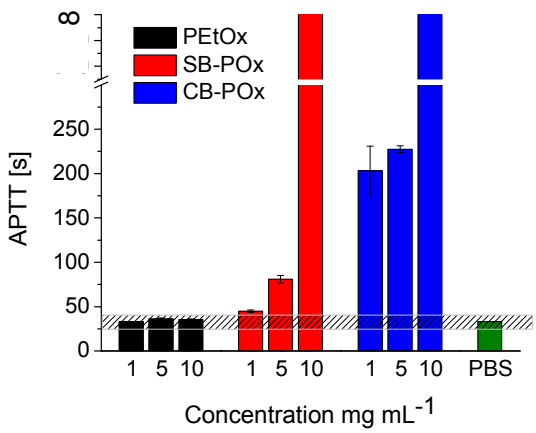

Figure 8. Effects of the polymers on the coagulation detected by A) The prothrombin time (PT) and B) and C) the activated partial thromboplastin time (APTT); after 5 min incubation. Experiments were run in triplicate and data are presented as the mean measured ± SD. Hatched area indicates the range of values judged as clinically normal.

Graphical Abstract

The hemocompatibility and cytotoxicity of zwitterionic poly(2-oxazoline)s are investigated.